



# DESIGNING AND MODELING OF COMPACT MICROSTRIP ANTENNAS USING NEW NANOCOMPOSITE MATERIALS

Mahdi Sharifi and Pejman Rezaei

Department of Electrical and Computer Engineering, Semnan University, Semnan, Iran

E-Mail: [m.sharifi@semnan.ac.ir](mailto:m.sharifi@semnan.ac.ir)

## ABSTRACT

This paper is the first applied study on the designing and modeling of compact microstrip antennas using new polymer nanocomposite magneto materials. New materials used in designing and modeling process of compact microstrip antenna are iron oxide polymer nanocomposite magnetic materials. Polymeric nanoparticles materials are created by iron oxide nanocomposite materials based on polydimethylsiloxane (PDMS). Nowadays, several researchers have been proposed magneto materials for minimizing and increasing the antennas bandwidth. Nevertheless, properties such as high loss and decreasing control in magnetic properties prevent the optimal performance of antennas. In addition, the incompatibility and high complexity prevents integration of conventional magnetic materials with antennas and standard fabrication processes at printed circuit boards and wafer levels. Additionally, low losses in magnetic nanoparticles accompany by the ease of integration of polymer nanocomposites in standard fabrication processes, suggests solutions to resolve any of the complications and concerns. So the present paper aim was designing and modeling of multilayer compact microstrip antenna using new polymer nanocomposite materials. In this paper, one multilayer antenna was created using new polymer nanocomposite materials based on PDMS with two similar microstrip antennas with different iron oxide nanoparticle concentrations of 80% and 30% by weight. The results showed that the polymer nanocomposite magnetic antenna performance not only in the antennas with different operating frequencies were achieved but the use of new polymer nanocomposite materials related with factors such as bandwidth and antenna performance and miniaturization.

**Keywords:** compact microstrip antennas, magnetic nanoparticles,  $\text{Fe}_3\text{O}_4$ -based polymer nanocomposite.

## 1. INTRODUCTION

The paper introduces the use of antennas with high-bandwidth on new magneto polymer nanocomposite materials. A compact antenna design is selected because of its high susceptibility to the substrate characteristics. This antenna has a microstrip configuration, and therefore the field interaction between the patch and the ground plane largely occurs in the substrate underneath the patch. [1]. Using newly polymer nanocomposites in microwave antennas, calls for the extraction of the intrinsic electrical properties of these materials, which is essential for the effective design and implementation of such devices. This process was developed by engineering a hybrid algorithm that combines time-domain techniques [2], frequency domain techniques [3] [4], with transmission line theory and conformal mapping methods [5] [6] [7].

Increasing the relative permittivity of the substrate material suffers from narrow bandwidth and low efficiency. These disadvantages are derived from the fact that the electric field remains in the high permittivity region and does not radiate. The low characteristic impedance in the high permittivity medium results in a problem for impedance matching as well [8]. On the contrary, magneto materials can reduce the antenna size with better antenna performance compared to the antenna on a high dielectric constant material [9]. According to the work of Hansen and Burke in [10], properly increasing the relative permeability leads to efficient size reduction of microstrip antennas. The impedance bandwidth can be retained after the miniaturization. Magnetic nanocomposites provide several advantages for antenna applications such as: a) low eddy current and domain wall

losses from nanoscale particle size and b) high frequency-stability because of various contributions from magnetic anisotropies that enhance the ferromagnetic resonance frequency. They also show enhanced permittivity with low loss for further antenna miniaturization and performance enhancement. They suffer from several limitations which result in suppression of permeability and enhanced damping, leading to higher losses over a broad frequency range [11].

Miniaturization of antenna typically leads to some level of performance degradation that cannot be avoided, even with the use of magneto materials. The performance of the antenna is going to suffer due to the reduction of its physical area and the increment of confined energy given the proximity of the metallization layers. In addition, the results presented are based in simulations under ideal circumstances, with the loss properties of the magnetic materials and the metallization layers being neglected. Undoubtedly, the aforementioned loss related properties would introduce a negative impact on the overall performance of any antenna implemented in real applications. [12]

Several antennas incorporating magneto substrates have been presented as an alternative approach, which continue to cope with issues related with high material losses [13]. This is particularly the case of an antenna configuration recently proposed by Erkmen et al in which ferrite layers with magnetic loss tangents of around 0.2 are implemented [14]. The effect of material losses has been decreased by maintaining a given distance between the printed antenna and the magnetic layer, with some drawbacks related to a high profile [13]. Namin *et*



*al.* [15] have proposed a methodology to design stacked-patch antennas based on magnetic substrates. In particular, they created an antenna in which the effective permeability and permittivity holds the same value, which is also referred as the matched magnetic condition. Under this circumstance, the impedance of the antenna is going to be equal to that of the free space. This unique property allows for a better impedance matching over the bandwidth of the antenna, thus decreasing any losses due to wave reflection within the antenna and the free space. Additionally, even with moderated values of permeability and permittivity of less than 5, considerable reductions in length, width and thickness were achieved [15].

## 2. METHOD

In this paper the fabrication process for multilayer flexible iron oxide nanocomposite materials based on polydimethylsiloxane antennas is presented, followed by description of integration of magnetic nanocomposite materials. Then, antenna performance is determined and the results are analyzed based on classical antenna theory.

The other two designs are constructed on a PDMS substrate with a cavity completely filled with Fe<sub>3</sub>O<sub>4</sub>-PDMS PNC at Fe<sub>3</sub>O<sub>4</sub> loading concentration of 30% and 80%. Three different multilayer microstrip antennas have been designed to explore the polymer nanocomposite (PNC) material. The first design consists of a pure Polydimethylsiloxane (PDMS) material between two flexible laminates that contain the copper metallization layers. In this paper, one multilayer antenna was created using new polymer nanocomposite materials based on PDMS with two similar microstrip antennas with different iron oxide nanoparticle concentrations of 80% and 30% by weight.

## 3. SYNTHESIS AND PROPERTIES OF POLYMER NANO-COMPOSITE MAGNETIC MATERIALS (PDMS-FE<sub>3</sub>O<sub>4</sub>)

Nanocomposite materials used in this paper are made of magnetite iron oxide. This material is a common magnetic iron oxide that has a cubic inverse spinel structure with oxygen forming a face centered cubic (FCC) closed packing, in which iron (Fe) cations occupy interstitial tetrahedral sites and octahedral sites [16] [17]. In the past, magnetite nanoparticles have been used as ferrofluids [16]. The nanoparticle synthesis follows a chemical procedure that requires a special pattern that provided a controlled and stable environment, necessary to obtain particles with the right chemical composition and a tight size distribution.

In this paper, iron oxide nanoparticles are synthesized via thermal decomposition reaction. Several chemicals are used for the synthesis of magnetite nanoparticles, including Iron (III) acetylacetonate (Fe(acac)<sub>3</sub>), oleylamine (technical grade, 70%), ethanol (200 proof, anhydrous, 99.5%), hexane (anhydrous, 95%), benzyl ether (98%) and oleic acid. All these chemicals were not modified to any extent and used as received. Following a standard chemical procedure, magnetic iron

oxide nanoparticles with an average size of 7 nm and coated with surfactants (oleylamine and oleic acid) are synthesized similar to what has been reported in [16] [18]-[19]. 10 mmol iron (III) acetylacetonate, 40 mL of oleylamine and 50 mL of benzyl ether are combined in a 700 ml. The mixture is magnetically stirred under a continuous flow of argon at room temperature for 5 minutes.

## 4. DESIGN AND MODELING OF MULTILAYER ANTENNA USING POLYMER MAGNETIC NANOCOMPOSITE MAGNETIC MATERIAL

In this paper the fabrication process for multilayer flexible iron oxide nanocomposite materials based on polydimethylsiloxane antennas is presented, followed by description of integration of magnetic nanocomposite materials. Then, antenna performance is determined and the results are analyzed based on classical antenna theory.

Three different multilayer microstrip antennas have been designed to explore the polymer nanocomposite (PNC) material. The first design consists of a pure Polydimethylsiloxane (PDMS) material between two flexible laminates that contain the copper metallization layers. The other two designs are constructed on a PDMS substrate with a cavity completely filled with Fe<sub>3</sub>O<sub>4</sub>-PDMS PNC at Fe<sub>3</sub>O<sub>4</sub> loading concentration of 30% and 80%.

### 4.1. Design of Multilayer Microstrip Antennas

At beginning, it is very difficult to conceive that given the geometrical configuration of a microstrip antenna can operate with minimal acceptable performance.

Given this characteristic, the microstrip patch antenna has been selected here because of its high sensitivity to the substrate material properties, derived from the high interaction within the patch and its ground plane throughout the substrate.

#### 4.1.1. First design: Multilayer patch antenna on plain PDMS material

A multilayer patch antenna on pure PDMS substrate has been designed to operate with a resonant frequency of 4GHz. This frequency has been selected in order to achieve a dual benefit: a convenient size to optimize the material resources and to facilitate antenna performance measurements.

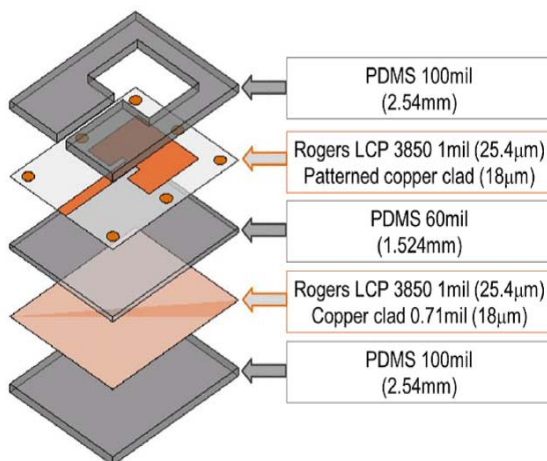
In order to retain an attractive radiation efficiency ( $\geq 90\%$ ), the thickness of the substrates has been selected to be around  $0.02 \lambda_0$  (1/50 of the signal wavelength in free space), as selected in [36] for a Teflon substrate which exhibits similar electrical characteristics. A thicker substrate selection would lead to improved radiation efficiency, but requires more substrate material. At 4GHz ( $\lambda_0 \sim 74.95\text{mm}$ ) a substrate with a thickness of 62mm (1.5748mm) is selected, which is equivalent to  $0.021\lambda_0$ .

Figure-1 depicts the 3D schematic diagram of the multilayer microstrip patch antenna assembly and identifies the constituent patterned layers and their

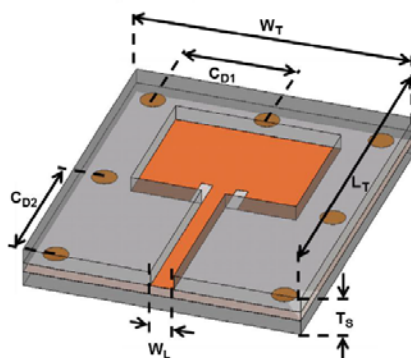


respective thicknesses. As shown, a 60mil (1.524mm) thick PDMS layer is sandwiched between two laminates featuring the antenna patch and the ground plane, respectively. Each laminate has a thickness of 1mil (25.4 $\mu$ m). The bottom side of antenna (i.e., underneath its ground plane) is totally covered by a 100mil (2.54mm) thick PDMS layer, while the top of the antenna is partially covered with a molded 100mil thick PDMS layer, with an opening over the antenna patch and microstrip line. PDMS is not desired on the top of the patch and microstrip as it will reduce the antenna efficiency.

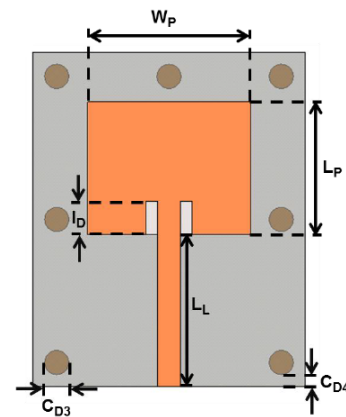
Encapsulation with PDMS helps keep the flexibility of the entire antenna assembly, without wrinkling the Rogers LCP laminates and copper clads, whenever the antenna is bent or flexed. Over the upper LCP laminate, seven small anchoring copper features have been located near the edges, in order to prevent the LCP substrate from sliding sideways when the antenna assembly is bent, and improve the bonding between PDMS layer and the flexible Rogers LCP laminate. It has been demonstrated by 3D electromagnetic simulations, that those features do not play any role in the antenna performance.



(a)



(b)



(c)

**Figure-1.** 3D schematic diagram of the multilayer microstrip patch antenna identifying all its layers with perspective and top view.

(a) Sub Figure-1, (b) Sub Figure-2, (c) Sub Figure-3

In this design, the total width, length and thickness dimensions of the patch antenna assembly were set to be  $W_T=1.77$ in (45mm),  $L_T=2.16$ in (55mm) and  $TS=262$ mil (6.65mm). Usually the width of the patch is assigned in the range of 1.25 to 1.75 times the length. In order to maintain the size is as small as possible, the minimum patch dimensions were chosen using the parametric relationship  $W_P=1.25L_P$ , resulting in  $W_P=1.07$  in (27.25mm),  $L_P=858.3$  mil (21.8mm) and  $ID=216.5$  mil (5.5mm), where the inset length (ID) is determined for optimum impedance matching.

#### 4.1.2. Second design: Multilayer patch antenna on PDMS-Fe<sub>3</sub>O<sub>4</sub> PNC substrate

A modified version of the multilayer patch antenna with PDMS-Fe<sub>3</sub>O<sub>4</sub> PNC substrate is presented herein. For ease of comparison, this antenna has also been set to work with a resonance frequency of 4GHz. Figure-2 presents the 3D schematic diagram of the multilayer microstrip patch antenna assembly while identifying all its layers and their respective thicknesses. As seen, this design differs from the previous in the incorporation of the PDMS-Fe<sub>3</sub>O<sub>4</sub> PNC underneath the patch and between the two laminates. Also, dimensions of the patch have been adjusted from those in the previous design to retain the same resonance frequency. Figure-2 shows the physical dimensions of the new antenna design. Now,  $W_P=777.56$  mil (19.75mm),  $L_P=622.05$  mil (15.8mm) and the insets are no longer needed ( $ID=0$ ). In addition, the dimensions of the PDMS-Fe<sub>3</sub>O<sub>4</sub> PNC filled cavity are  $W_N=866.14$  mil (22mm),  $L_N=669.29$  mil (17mm) and with the same thickness of the PDMS substrate 60 mil (1.524mm). The rest of the physical parameters are kept the same as in the previous design. As noted, since the resonance frequency of the antenna has been kept the same, then size comparison between the antennas could be accomplished based on the areas of the antenna patch in different designs.

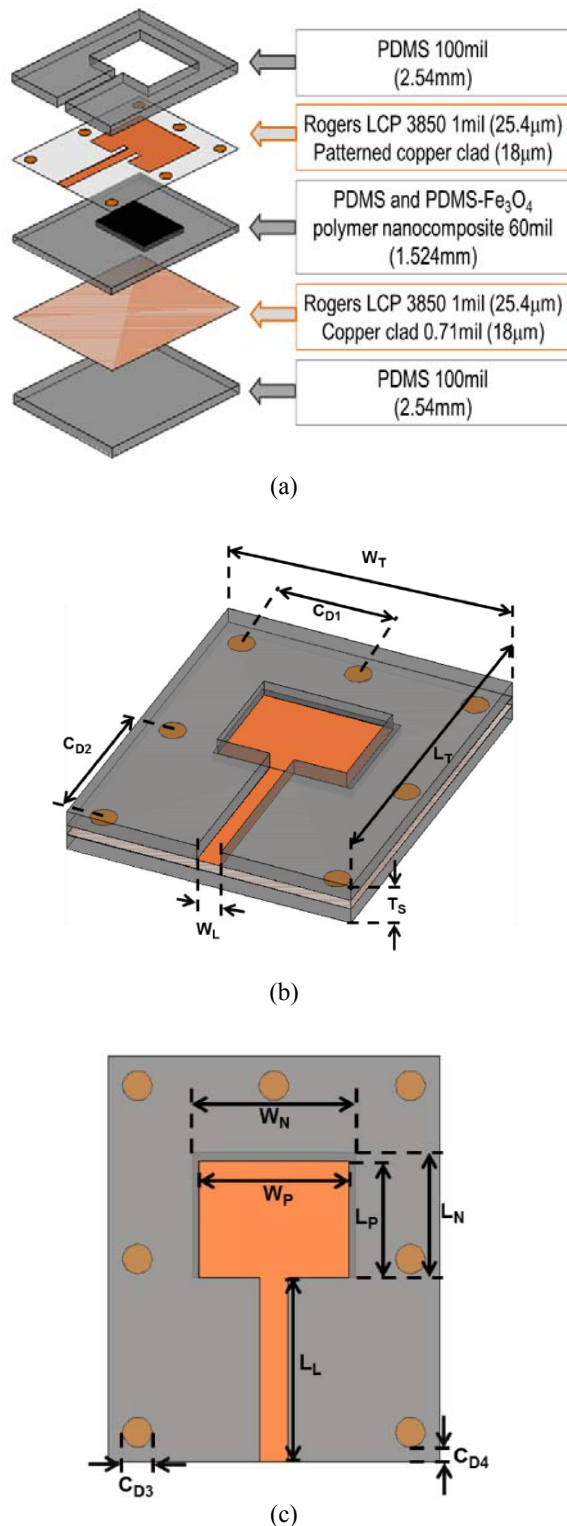


**Figure-2.** 3D schematic of the multilayer microstrip patch antenna with a cavity embedded completely filled with PDMS-Fe<sub>3</sub>O<sub>4</sub> PNC with perspective and top view  
(a) Sub Figure-1, (b) Sub Figure-2, (c) Sub Figure-3

In the Figure-2/Sub Figure-3 the top-view of the assembled multilayer Antenna includes a PDMS-Fe<sub>3</sub>O<sub>4</sub> PNC filled cavity underneath the antenna patch both figures identify key features and dimension parameters. Note that  $W_N$  and  $L_N$  describe the dimensions of the embedded PNC layer.

#### 4.2. Multilayer patch antenna on hybrid PDMS/Fe<sub>3</sub>O<sub>4</sub>-PDMS substrate

For this design, both metallization layers (ground plane and patch) are constructed on flexible laminates following the same process steps. As a layer of PDMS-Fe<sub>3</sub>O<sub>4</sub> PNC is incorporated in this design, the fabrication process of the multilayer array is modified to facilitate the integration of the new layer. Aside from the cavity built at its center, this PDMS layer is cut smaller in area and aligned to the center of the mold, which will be bonded to the multilayer stack by molding of the next PDMS layer. PDMS/Fe<sub>3</sub>O<sub>4</sub> PNC is poured in the cavity followed by evaporation of the solvent and refilling until the cavity is completely filled. After the cavity is filled, the PNC is planarized using a spatula. A top-view photo of the finalized patch antenna on PDMS-Fe<sub>3</sub>O<sub>4</sub> PNC multilayer substrate is shown in Figure-3.

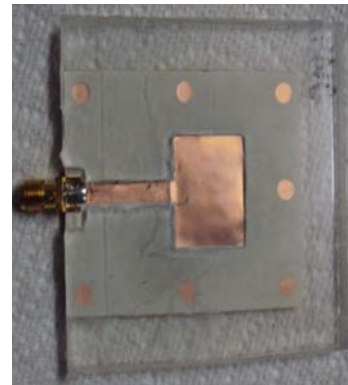


**Figure-3.** Top-view photo of multilayer patch antenna constructed on PDMS-Fe<sub>3</sub>O<sub>4</sub> PNC.

PDMS in the upper layer on the top of the patch and the microstrip feed line has been removed, and the port has been terminated with a coaxial SMA connector. The embedded cavity filled with PNC is not visible as it is hidden underneath the upper Rogers LCP laminate with the patterned antenna patch.

#### 4.3. Experimental results

As mentioned before, four different designs with different loading of Fe<sub>3</sub>O<sub>4</sub> nanoparticles have been simulated and measured. The return loss and radiation pattern of all the antennas are measured and then compared with the results obtained. The PDMS antenna is used as the reference for performance comparison purposes with the other three remaining designs, which include the usage of PDMS-Fe<sub>3</sub>O<sub>4</sub> PNCs at different Fe<sub>3</sub>O<sub>4</sub> weight concentrations of 80% and 30%, respectively. For organization purposes, each antenna is





analyzed independently and then compared in the final sub-section.

#### 4.3.1 Pure PDMS-based antenna (without fillers)

Simulated and measured return losses for the pure PDMS-based multilayer patch antenna are shown in Figure-4. These results show measured and simulated resonance frequencies of 3.931GHz and 4.002GHz, respectively. The difference in the resonance frequencies is only of 71MHz or 1.77%, which confirms that an excellent extraction of the PDMS electrical properties has been implemented. The small frequency offset may be introduced during the simulation (the approximations of the finite element method) and the inclusion of elements such as the SMA feeding connector.

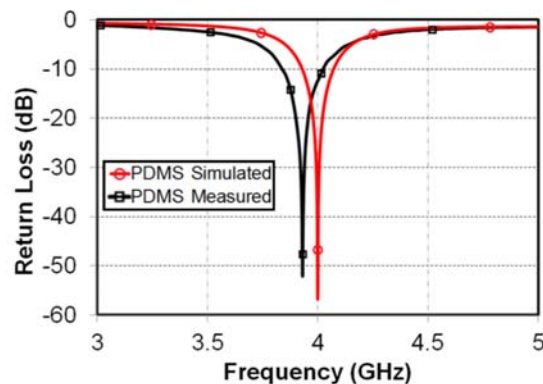


**Figure-4.** Measured and simulated return loss for the patch antenna on pure PDMS-based molded multilayer substrate, showing acceptable agreement in resonance frequencies.

#### 4.3.2. Multilayer microstrip patch antenna with PDMS-Fe<sub>3</sub>O<sub>4</sub> PNC filler at 80% and 30% w.t. concentration

Simulated and measured return losses for the multilayer patch antenna with PDMS-Fe<sub>3</sub>O<sub>4</sub> PNC at 80% w.t. concentration are shown in Figure-5/SubFigure-1. An excellent agreement between resonance frequency and bandwidth can be observed, however some discrepancy in the return loss is exhibited, which may be ascribed to different impedance matching conditions. As mentioned before, the inclusion of the SMA feeding connector can add some variations to the response of the measured antenna, as well as the preciseness of the finite element method for the antenna simulation.

Return loss for the multilayer patch antenna with PDMS-Fe<sub>3</sub>O<sub>4</sub> PNC at 30% w.t. is shown in Figure-5/SubFigure-2, presenting an excellent agreement between measured and simulated results. Minor discrepancies are found in the impedance matching of the antenna, but good matching between the frequency responses obtained for both approaches.

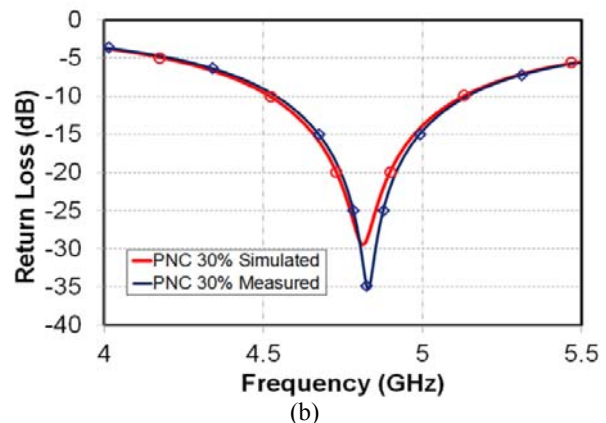
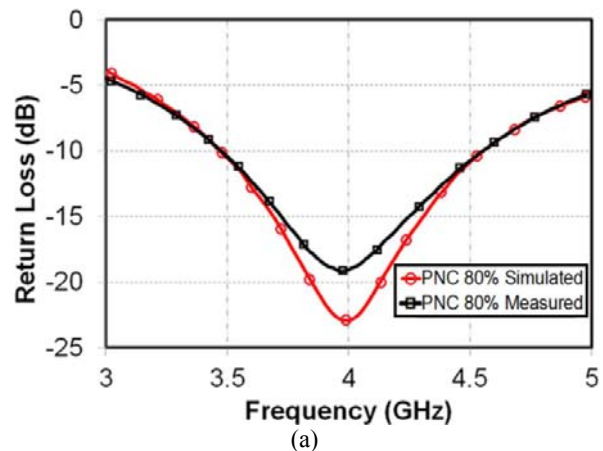


**Figure-5.** Return loss for microstrip the multilayer patch antenna with PDMS-Fe<sub>3</sub>O<sub>4</sub> PNC at 80% and 30% w.t. (a) Sub Figure-1, (b) Sub Figure-2

#### 4.4. Performance comparison of multilayer patch antennas built on PDMS-Fe<sub>3</sub>O<sub>4</sub>

A systematic analysis of the performance of the antennas is developed, comparing the measurement results obtained from the different designs (PDMS, 80% and 30% PNC). The primary antenna performance metrics, such as return loss, antenna radiation pattern, maximum gain, directivity and antenna efficiency are analyzed and explored for each design. Initially, comparisons between the as-constructed antennas are presented without the presence of any biasing magnetic field. Subsequently, comparisons are carried out among the measurement results obtained while a DC biasing magnetic field is applied to the antennas through the employment of a permanent magnet in close proximity to the embedded PNC material.

#### 4.5. Performance of PDMS-Fe<sub>3</sub>O<sub>4</sub> PNC multilayer antennas without externally applied DC biasing magnetic field

Figure-6 compares the return losses multilayer antennas constructed on the pure PDMS substrate and the PDMS-Fe<sub>3</sub>O<sub>4</sub> PNC at 80% w.t. antennas substrate. Both



devices were designed to operate at 4GHz, resulting in resonance frequencies of 3.931GHz and 3.981GHz for the PDMS and 80% PNC designs, respectively. By direct comparison of the return loss responses, the 80% PNC antenna presents an attractive widened bandwidth of 26.95% (1072.5MHz), which is 5.7 times wider than the bandwidth of 4.7% (185MHz) of its plain PDMS counterpart.

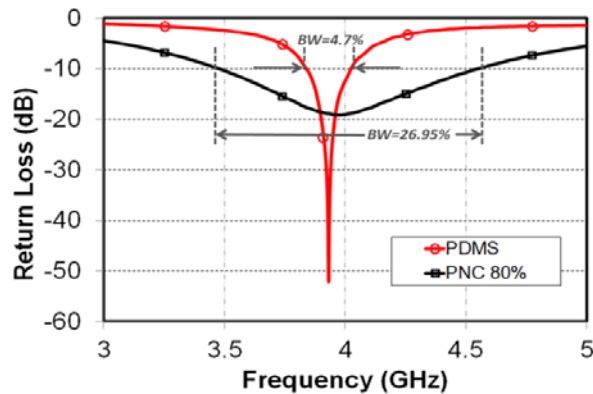


**Figure-6.** Measured return losses for plain PDMS and 80% w.t. PDMS-Fe<sub>3</sub>O<sub>4</sub> PNC multilayer patch antennas.

However, the pure PDMS patch obtained an acceptable efficiency of 51%, which is much better than the 12.2% efficiency obtained by the 80% PNC antenna. Although an increased bandwidth is expected, caused by the magneto107 properties of the 80% PNC substrate, such a great difference in the bandwidth is mainly caused by the high loss property introduced by the PNC material, which lowers the antenna quality factor and leads to an increased bandwidth at expenses of degrading the antenna efficiency.

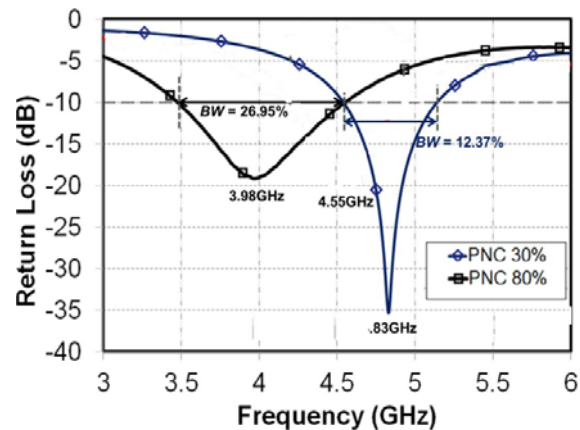


**Figure-7.** Measured return losses of PDMS-Fe<sub>3</sub>O<sub>4</sub> PNC multilayer patch antennas at 30% and 80% w.t. concentrations.

Figure-7 shows the measured return losses of three multilayer patch antennas with embedded PDMS-Fe<sub>3</sub>O<sub>4</sub> PNCs at different particle loading concentration (80% and 30%). All these multilayer patch antennas have the same physical dimensions. Also Table-1 presents a comparison of measured key performance metrics for all four multilayer patch antenna designs without any applied DC biasing magnetic field. The antenna designs are discriminated by the PNC materials used as the cavity filler underneath the antenna patch. In addition, the antenna bandwidth and efficiency are strongly affected by the magnetic losses presented in the substrate fillers, properties which are inherent to the concentration of magnetite nanoparticles in the PNC.

**Table-1.** Multilayer patch antennas and their relevant properties without any applied biasing magnetic field.

Antenna design	Resonance frequency (GHz)	Bandwidth (MHz)	Maximum gain (dBi)	Efficiency
PDMS	3.931	185 (4.7%)	5.681	50.74%
PDMS-Fe <sub>3</sub> O <sub>4</sub> 80% PNC	3.981	1072.5 (26.95%)	-1.428	12.23%
PDMS-Fe <sub>3</sub> O <sub>4</sub> 30% PNC	4.832	597.5 (12.37%)	2.003	23.98%

Increasing the Fe<sub>3</sub>O<sub>4</sub> nanoparticle concentration also raises the PNC material effective permeability thus leading to a wider antenna bandwidth. However, this is accompanied by the increase of additional material losses, which contributes to a significant increase of the bandwidth and a degradation of the antenna efficiency. Fortunately, the additional losses and the antenna gain/efficiency degradation can be addressed by means of externally applied DC biasing magnetic fields. Unfortunately, given the large variation of the strength of the magnetic field as a function of the position, it is impossible to precisely predict the values of permittivity

and permeability of the PNCs under the influence the biasing magnetic field produced by the Neodymium magnet array. Nevertheless, it is anticipated that the influence of the biasing magnetic field is favorable to the decrease of the loss tangent of the PNCs as well as the increment of its relative permeability and permittivity, thus making a positive impact on the antenna performance.

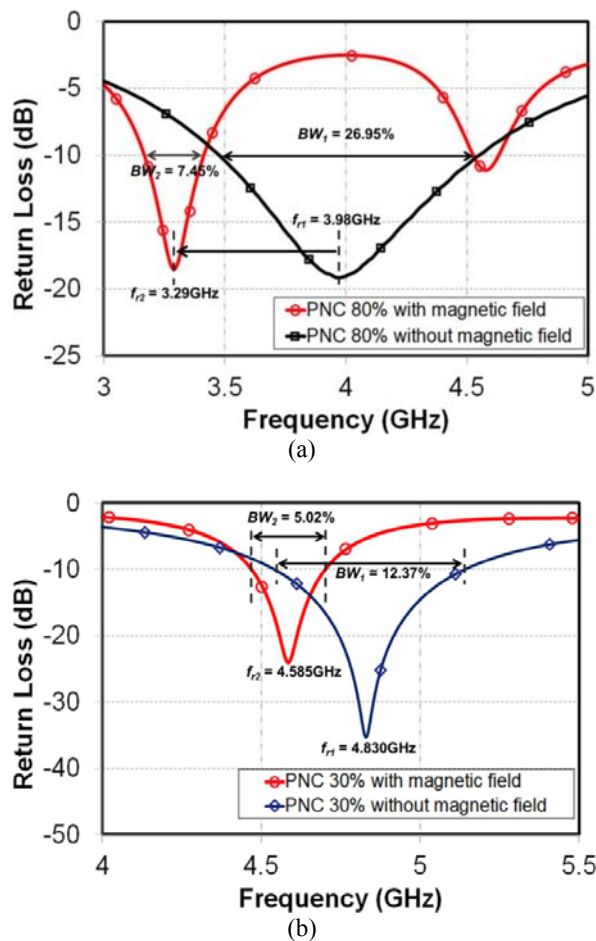


**Figure-8.** Measured returns loss of PDMS-Fe<sub>3</sub>O<sub>4</sub> PNC multilayer patch antenna at 80% w.t. and 30% concentration with and without applied DC biasing magnetic field.

(a) Sub Figure-1, (b) Sub Figure-2

Figure-8/Sub Figure-1 presents the return loss of the PDMS-Fe<sub>3</sub>O<sub>4</sub> PNC multilayer patch antenna at 80% w.t. concentration, measured under the action of the DC magnetic field provided by the Neodymium magnet array and directly compared to the return loss of the same antenna in absence of magnetic field. As shown, the bandwidth has been reduced considerably from 26.95% to 7.45% under the influence of magnetic field. Although the magneto nature of the PNC material has been retained, there is still a field-induced bandwidth reduction, which corresponds to a decrease in the combined magnetic losses in the PNC. Moreover, the resonance frequency has been

lowered from 3.98GHz to 3.29GHz when magnetic field is applied. As expected, the resonance frequency has dropped to a lower value because of an increase in the product of the relative permeability and permittivity under the influence of DC biasing magnetic field.

Figure-8/Sub Figure-2 presents a better contrast of the antenna gain with and without applied magnetic field versus frequency. In this plot, it can be seen that the gain has increased from 2.003dBi at 4.83GHz without biasing field to 5.085dB at 4.585GHz in the presence of biasing field, which represents an effective gain increase of 3.082dB or equivalent to 2 times the gain.

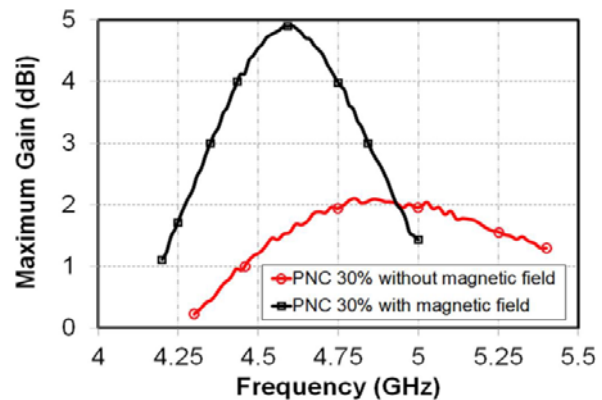


**Figure-9.** Measured gain of PDMS-Fe<sub>3</sub>O<sub>4</sub> PNC multilayer patch antenna at 30% w.t. concentration with and without applied magnetic field.

The effective miniaturization percentage and miniaturization factor for all three magneto PNC antennas, achieved by the application of the external biasing magnetic field. The results are summarized in the Table-2, which also compares the antenna performance parameters for all four multilayer patch antenna designs. All the PNC antennas have achieved excellent miniaturization factors as compared to the size of the plain PDMS antenna. 30% PNC antenna only exhibited a slightly increased bandwidth, whereas the 30% PNC and 80% PNC antennas have both been demonstrated a notable bandwidth enhancement effect. Among all three PNC designs, the 30% PNC antenna has achieved the best efficiency which is almost comparable to the efficiency of the pure PDMS counterpart. Nevertheless, the antenna efficiencies have been improved substantially for all the PNC antenna designs through the application of external DC-biasing magnetic field generated by a stacked magnet array.

**Table-2.** Antenna parameters of all the multilayer patch antennas with PNC-filled substrates and applied external DC biasing magnetic field. (The plain PDMS antenna design is included as the reference device for comparison purposes.).

Antenna design	Resonance frequency (GHz)	Bandwidth (MHz)	Maximum gain (dBi)	Efficiency
PDMS	3.931	185 (4.7%)	5.681	50.74%
PDMS-Fe <sub>3</sub> O <sub>4</sub> 80% PNC	3.298	245 (7.45%)	2.12	31.28%
PDMS-Fe <sub>3</sub> O <sub>4</sub> 30% PNC	4.585	230 (5.02%)	5.085	40.49%

A gain of 5.085 dBi is obtained for the 30% PNC antenna design, which is similar to the 5.681 dBi obtained for the plain PDMS antenna. This result demonstrates that miniaturized antennas with enhanced bandwidth can be implemented by the employments of low-loss polymer nanocomposites with monodispersed super paramagnetic nanoparticles, without a considerable degradation in the overall antenna radiation performance. As a matter of fact, there is a direct correlation between the physical area of the antenna and its highest achievable performance (gain, efficiency, etc.). The antenna with plain PDMS substrate presents larger dimensions than the PNC-based antenna designs, thus a direct comparison between the measured gains obtained from the different elaborated antennas could be ambivalent. Nevertheless, a direct comparison is made in this case to describe that a certain acceptable gain can be realized for antennas that employ magneto PNC materials as substrate fillers.

## 5. DISCUSSIONS AND CONCLUSIONS

This research has presented the usage of magnetite-based magneto polymer nanocomposites for the implementation of miniaturized multilayer patch antennas. Four different patch antenna designs were systematically explored. Each one of the PDMS-based design has a different loading concentration of superparamagnetic nanoparticles (from 0% to 80%).

The performance of the constructed antennas was measured with and without externally applied DC biasing magnetic field. Comparisons between the different designs were thoroughly conducted to demonstrate the correlation between the nanoparticle loading concentration presented in the polymer nanocomposites and the corresponding resultant magnetic properties.

Antenna miniaturization up to 57% and antenna bandwidth increase of 58% (from 4.7% to 7.45%) have been successfully demonstrated, while retaining an acceptable antenna gain by the employment of PDMS-Fe<sub>3</sub>O<sub>4</sub> PNC with 80% w.t. concentration. Furthermore, the reduction of the loading concentration of the superparamagnetic nanoparticles in the PNC (e.g. 80% w.t. PNC and 30% w.t. PNC) decreased the magnetic loss properties, then resulting in the enhancement of the antenna gain, up to the value close to that achieved by its pure PDMS counterpart. Beyond acknowledging that the reduction of nanoparticle loading does decrease the permeability of the resultant PNC, thereby reducing both bandwidth miniaturization factor of the multilayer

antenna, it is paramount to notice that resulting magneto characteristics of the PDMS-Fe<sub>3</sub>O<sub>4</sub> nanocomposite materials with low nanoparticle concentrations, do offer superior electrical properties when compared to pure PDMS substrates. For instance, the antenna with embedded PDMS-Fe<sub>3</sub>O<sub>4</sub> PNC at 30% w.t. has exhibited a gain of 5.085 dBi, similar to the measured gain of 5.095 dBi of the pure PDMS antenna. Additionally, the antenna with the PNC at 30% w.t. presented slightly increased bandwidth of 5.02% (as compared to the 4.7% for pure PDMS counterpart), together with a significant miniaturization of 39.5%, which enables 1.65 times smaller antenna dimensions.

In conclusion, the novelty of this paper is the fact that it represents the first known successful attempt when PDMS-Fe<sub>3</sub>O<sub>4</sub> magneto polymer nanocomposites have been effectively employed for the miniaturization and bandwidth enhancement of microstrip patch antennas.

Finally, the demonstration of tunability of the antenna characteristics (i.e., resonance frequency and radiation properties), under externally applied DC magnetic fields generated by permanent magnets, opens alternate approaches for further research and implementation of reconfigurable antennas as well as tunable antenna arrays.

The methodologies and experiments developed in this paper can be used as the baseline for the implementation of multilayer planar antennas that employ low-loss superparamagnetic polymer nanocomposites systems as substrates.

New magneto polymer nanocomposites can be developed by selecting different polymer matrices and nanoparticles. The selection of a polymer with very low losses will help improve antenna performance. Factors such as the compatibility with the nanoparticle system and the solvents used for the nanoparticle suspension should be considered. Furthermore, magneto polymer nanocomposites may be used in other antenna topologies in order to achieve increased miniaturization and maximize the antenna performance (i.e., antenna gain, bandwidth), while taking full advantage of the properties of these new polymeric materials.

Finally, the magneto PNC materials developed in this work can be investigated simultaneously with Electromagnetic Band Gap Structures and Frequency Selective Surfaces. The proper implementation of magneto PNC in such structures may help improve their operational frequency range and provide additional miniaturization.





## REFERENCES

- [1] Cesar A. Morales. 2011. Magneto-Dielectric Polymer Nanocomposite Engineered Substrate for RF and Microwave Antennas. University of South Florida Scholar Commons.
- [2] A. M. Nicolson and G. F. Ross. 1970. Measurement of the intrinsic properties of materials by time-domain techniques. *IEEE Transactions on Instrumentation and Measurement*. IM-19(11): 377-382.
- [3] W. B. Weir. 1974. Automatic measurement of complex dielectric constant and permeability at microwave frequencies. *Proceedings of the IEEE*. 62(1): 33-36.
- [4] J. Barker-Jarvis, E. Vanzura and W. Kissick. 1990. Improved technique for determining complex permittivity with the transmission/reflection method. *IEEE Transactions on Microwave Theory and Techniques*. 38(8): 1096-1103.
- [5] E. Hammerstad and O. Jensen. 1980. Accurate models for microstrip computeraided design. in *IEEE MTT-S International Microwave Symposium Digest*. pp. 407-409.
- [6] M. Kirschning and R. H. Jansen. 1982. Accurate model for effective dielectric constant of microstrip with validity up to millimetre-wave frequencies. *Electronics Letters*. 18(6): 272-273.
- [7] E. Yamashita. 1968. Variational method for the analysis of microstrip-like transmission lines. *IEEE Transactions on Microwave Theory and Techniques*. MTT-16(8): 529-535.
- [8] H. Mosallaei, K. Sarabandi. 2004. Magneto-dielectrics in electromagnetics: concept and applications. *IEEE Trans. Antennas Propagat.* 52(6): 1558-1567.
- [9] P. Ikonen, K. Rozanov, A. Osipov, P. Alitalo, S. Tretyakov. 2006. Magnetodielectric substrates in antenna miniaturization: potential and limitations. *IEEE Trans. Antennas Propagat.* 54(11): 3391-3398.
- [10] R. C. Hansen, M. Burke. 2000. Antennas with magneto-dielectrics. *Microwave and Optical Tech. Lett.* 26(2): 75-78.
- [11] P. Markondeya Raj, P. Chakrabortu, Himani Sharma, Kyu Han, S. Gandhi, S. Sitaraman, Madhavan Swaminathan, Rao Tummala. 2014. Tunable and Miniaturized RF Components with Nanocomposite and Nanolayered Dielectrics. *IEEE Nanotechnol. Conf. (IEEE NANO)*. pp. 27-31.
- [12] F. Namin, T. G. Spence, D. H. Werner and E. Semouchkina. 2010. Broadband, Miniaturized Stacked-Patch Antennas for L-Band Operation Based on Magneto-Dielectric Substrates. *IEEE Transactions on Antennas and Propagation*. 58(9): 2817-2822.
- [13] P. Markondeya Raj, Himani Sharma, Dibyajit Mishra, K. P. Murali, Kyu Han, Madhavan Swaminathan, Rao Tummala. 2012. Nanomagnetics for High-Performance, Miniaturized Power, and RF Components. *IEEE Nanotechnology magazine*. 6(3): 18-23.
- [14] Kyu Han, Madhavan Swaminathan, P. Markondeya Raj, Himani Sharma, K.P. Murali, Rao Tummala, Vijay Nair. 2012. Extraction of electrical properties of nanomagnetic materials through meander-shaped inductor and inverted-F antenna structures. *Proc. IEEE Electronic Components and Technol. Conf. (ECTC)*. pp. 1808-1813.
- [15] F. Namin, T. G. Spence, D. H. Werner and E. Semouchkina. 2010. Broadband, Miniaturized Stacked-Patch Antennas for L-Band Operation Based on Magneto-Dielectric Substrates. *IEEE Transactions on Antennas and Propagation*. 58(9): 2817-2822.
- [16] S. Sun and H. Zeng. 2002. Size-Controlled Synthesis of Magnetite Nanoparticles. *Journal of the American Chemical Society*. 124(28): 8204-8205.
- [17] R.M. Cornell, U. Schwertmann. 1996. *The Iron Oxides: Structure, Properties, Reactions, Occurrence and Uses*. VCH, New York. pp. 28-29.
- [18] L. Fu, V. P. Dravid and D. L. Johnson. 2001. Self-assembled (SA) bilayer molecular coating on magnetic nanoparticles. *Applied Surface Science*. 181(1-2): 173-178, 9/3.
- [19] J. Gass, P. Poddar, J. Almand, S. Srinath and H. Srikant. 2006. Super paramagnetic Polymer Nanocomposites with Uniform Fe<sub>3</sub>O<sub>4</sub> Nanoparticle Dispersions. *Advanced Functional Materials*. 16(1): 71-75.